

# PHOTOELECTRON SPECTROSCOPY OF RADICALS



**Shibu E S**

**(CY07D011)**

**Uday Baskar Rao**

**(CY06D028)**

**Jasmine Maria Joseph**

**(CY07D010)**

**Goutam Kumar Kole**

**(CY05C008)**

**Puran Kumar De**

**(CY05C013)**

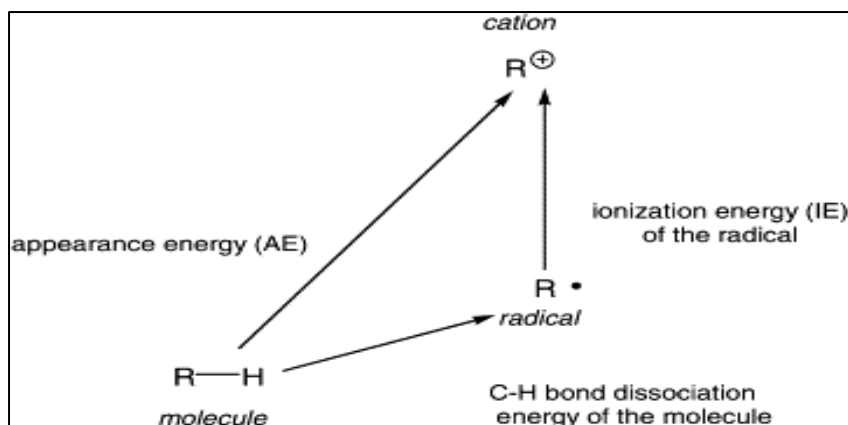
# PHOTOELECTRON SPECTROSCOPY OF RADICALS

## Introduction

Photoelectron spectroscopy has its basis on Einstein's photoelectric effect. The photoelectron spectroscopic techniques involve the ejection of an electron by ionizing the atom or molecule, M with a beam of monoenergetic photons. It can be represented as follows.



$$\text{I. E.} = h\nu - \text{K. E.} (e^-); \quad (\text{Eint} = 0)$$



In this manuscript we are discussing mainly the PES of NO, OH, Alkoxy, and Allyl radicals. Being the smallest hydrocarbon with an odd number of  $\pi$ -centers and due to the presence of 'allylic stabilization' or 'allylic rearrangement', the Allyl radical is a typical prototype for the understanding of  $\pi$ -stabilization effects.

## GENERATION OF RADICALS

The generation of radicals in sufficient number density is a difficult task. There are three different methods to generate the radicals in PES including,

- Flash Pyrolysis
- Photolysis
- Electric discharge

## Pyrolysis

Pyrolysis though an old technique, is used in PES for generating radicals. Earlier, an effusive flow of vapor at low pressure was passed through a heated tube coupled directly to the ionization region of the spectrometer. BUT here there was a problem of radical distraction by secondary processes. By the mid of 1980s, this problem was solved using high-pressure flash pyrolysis source coupled with a supersonic expansion. In this, an electrically heated silicon carbide tube having a length of 10-20mm and a diameter of 1 mm is mounted onto a molecular beam source with an orifice of 0.6 to 0.8 mm. A suitable precursor, diluted in 1-2 bar of a rare gas is expanded through the nozzle in to the vacuum. A wide variety of radicals are produced in high density.

## Photolysis

This is a common method for the generation of radicals in high density. In this technique a laser beam is used to excite the precursor molecule electronically and dissociate it into a radical of interest and a second fragment. Iodides are often used as precursors for organic radicals because they generally have dissociative states in the UV region, which can be conveniently excited with the fourth harmonic of a Nd: YAG laser at 266 nm or a 248 nm excimer laser. By focusing the laser a few mm behind the pulsed valve orifice, photolysis is coupled to supersonic beams (Figure 1)

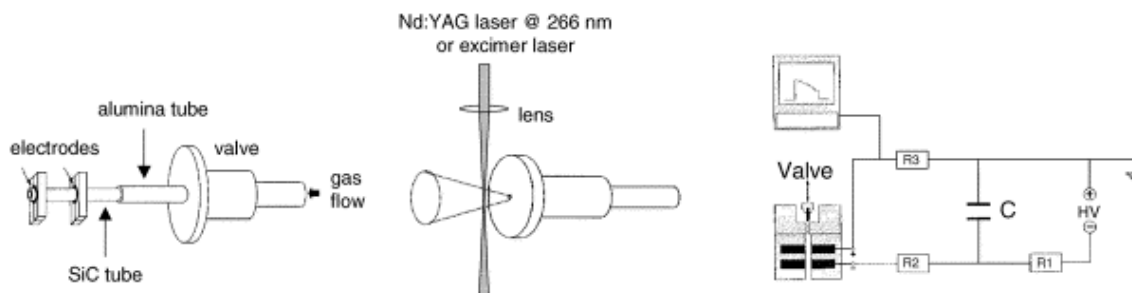


**Figure 1-** the schematic diagram for Flash photolysis, Pyrolysis, and electric discharge.

Photolysis method is expensive due to the less availability of proper lasers, which can efficiently eject photons of desired intensity.

## Electric Discharge

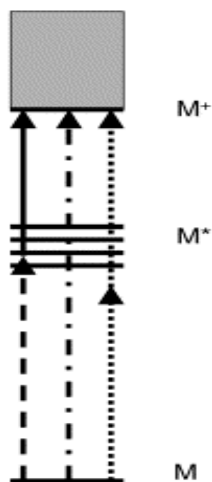
Another way to generate radicals is giving electric discharge. Good yield radicals are produced by combining electric discharge with supersonic jet sources. A typical setup for a pulsed electric discharge is shown in the right-hand trace of Figure 1. An insulating Teflon block with a small channel, containing two electrodes, is mounted onto the pulsed valve. When the valve opens, and the molecules pass through the channel, the circuit is closed and bonds in the precursor are cleaved in the occurring discharge. The problem with the discharge sources is the lack of selectivity and the presence of many side products. Although discharge sources have been employed in conventional PES, no prominent results are there with ZEKE spectra.

## OPTICAL EXCITATION OF THE MOLECULE

The three important techniques to optically excite molecule into high-lying Rydberg states are,

- One-Photon VUV excitation
- Resonant
- Non-resonant

All of these three have been applied to study radicals by ZEKE-spectroscopy.



For most of the polyatomic radicals having low I E, one photon excitation by tunable VUV radiation is used as a method of excitation. But the production of VUV that is tunable over a large enough range to sample a number of vibrational states on a laboratory scale is difficult. For that a synchrotron light source can be used and it can be used for VUV and XUV light tunable over a wide range for ZEKE-spectroscopy. In Resonant multiphoton excitation, the 1st laser, fixed at a resonant excitation frequency, populates selected Intermediate vibronic states. 2nd tunable laser subsequently promotes the molecule into a high-lying Rydberg state. Intermediate state selection reduces number of lines and thus the complexity of spectrum. But in Non-resonant multiphoton excitation, only one tunable laser is required.

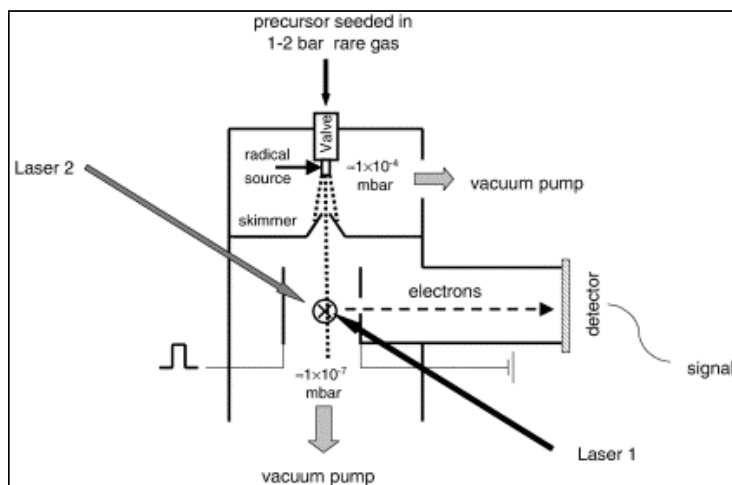


**Figure 3-** The schematic representation of the experimental setup.

A typical set-up for the ZEKE-spectroscopy is depicted in figure 3. A precursor, diluted in 1-2 bar of a rare gas, is expanded through a pulsed valve into the vacuum. A radical source is attached to the faceplate of the valve. The radicals formed are adiabatically cooled by collisions with the carrier gas and enter the collision free zone where the radicals are frozen and no further interactions take place and through a skimmer the beam enters the second chamber, where the spectroscopic experiment is performed. One or two laser beams for excitation and ionization crosses the molecular beam in the ionization chamber. A negative pulse (typically, but not necessarily, between 1 and 10 V/cm) is applied to one of the electrodes after a delay of 1  $\mu$ s. Electrons are

accelerated towards a detector and the Rydberg states are field ionized. The signals are recorded as a function of the wavelength.

### NO Radicals.

The first molecule to be investigated by ZEKE- spectroscopy which a vast amount of experiments were carried out over the last 15 years was NO. The ZEKE-spectrum of the  $X^+2\Sigma^+$  cationic ground state of NO is shown in figure 4. This is obtained by the non-resonant two-photon ionization from the  $^2\Pi_{1/2}$  electronic ground state. A theoretical spectrum is also shown, assuming a rotational temperature of 2.5 K. Due to the low temperature only transitions originating from the two lowest rotational levels,  $J''=1/2$  and  $J''=3/2$  are observed. The appearance of transitions into ionic rotational states up to  $N^+=4$  shows the more relaxed angular momentum selection rules in PES. The maximum change expected in angular momentum,  $\Delta J_{\max}$ , is  $\Delta J_{\max}=\ell+3/2$ . The unpaired electron in the  $^2\Pi_{1/2}$  electronic ground state of NO was calculated to be an electron predominately of d-character. This can be ejected into the  $\ell=s$ -, d- or g-continuum and a  $\Delta J_{\max}$  of 11/2 is calculated. The maximum change observed in the spectrum is  $\Delta J_{\max}=7/2$ . But weak  $\Delta J_{\max}=9/2$  transitions were also observed for higher  $J''$  states, but only populated in a warmer spectra. We can thus conclude that the electron is predominately excited to the s- and d-continuum channels.

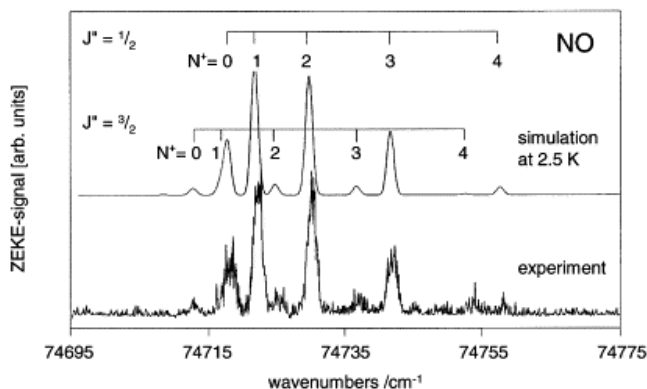


**Figure 4-** Shows the ZEKE spectrum of NO, recorded by non-resonant two photon excitation from the electronic ground state with simulation assuming a rotation temperature of 2.5 K given for comparison.

### OH Radical

As the hydroxyl radical plays an important role in the chemistry of the Earth's atmosphere, combustion processes, and the interstellar medium, the PES of this is also important.

The ground state electronic configuration of OH is



The **He-I** (21.22 eV) photoelectron spectrum of OH, prepared via the F+H<sub>2</sub>O reaction, gives all three bands associated with the (1  $\sigma$ )<sup>-1</sup> ionization. They exhibit nonbonding characteristics with adiabatic ionization energies (AIES) of 13.01, 15.17, and 16.61 eV. For the (3  $\sigma$ )<sup>-1</sup> ionization, due to the poor transmission of the spectrometer above 18.0 eV which prevented observation of the OH<sup>+</sup> (*c* 1 $\sigma$ )  $\leftarrow$  OH (*X*<sup>2</sup> $\sigma$ ) band only the OH<sup>+</sup> (*A* 3 $\sigma$ )  $\leftarrow$  OH (*X*<sup>2</sup> $\sigma$ ) band was observed. As predicted the OH<sup>+</sup> (*A* 3 $\sigma$ )  $\leftarrow$  OH (*X*<sup>2</sup> $\sigma$ ) band (AIE-16.48 eV) is wide and the vibrational separations are smaller than in the ground state neutral molecule.

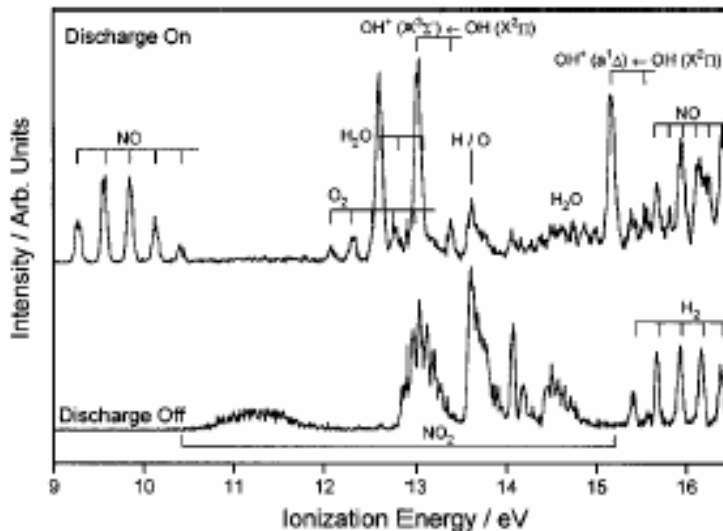


**Figure 5.** Photoelectron spectra recorded for the reaction mixture H<sub>2</sub>/He/NO<sub>2</sub> with the microwave discharge on and off, at a photon energy of 21.22 eV. NO<sub>2</sub> was added to the H<sub>2</sub>/He mixture; 30 cm after the H<sub>2</sub>/He discharge and; 3 cm above the photon beam.

### Methyl Radicals

The methyl radical which is an important intermediate in the growth of diamond thin films by CVD and in hydrocarbon combustion, was the first polyatomic radical to be studied by ZEKE-spectroscopy with rotational resolution. Methyl radical is formed by flash pyrolysis of azomethane, CH<sub>3</sub>NNCH<sub>3</sub> in Ar at around 1300 K. ZEKE-spectra were recorded using tunable VUV radiation around 126 nm produced by resonant difference-frequency mixing in Kr via the 5p<sub>5/2</sub> $\leftarrow$ 4p two-photon transition at 2 $\times$ 216.67 nm. Figure 6 shows the comparison between the experimental spectrum and a spectrum obtained from ab initio calculations, assuming a rotational temperature of 250 K.

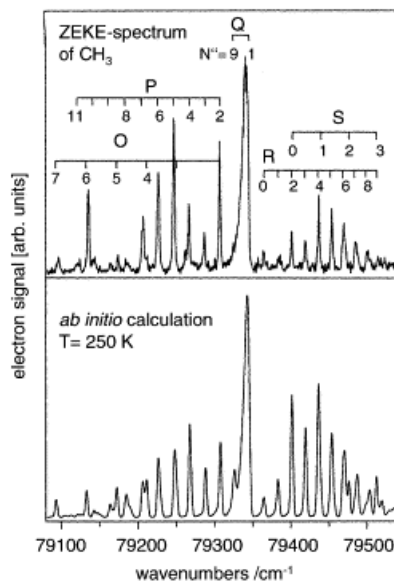


**Figure 6-** The rotationally resolved one-photon ZEKE-spectrum of methyl radical. The lowest trace shows a simulation based on ab initio calculations.

The agreement between theory and experiment is excellent. The X<sup>2</sup>A<sub>1</sub>' of the cation is planar as the <sup>2</sup>A<sub>2</sub>" ground state of the neutral and can be described as an oblate rotor. The different branches are labeled with respect to the  $\Delta N=N^+-N''$  quantum number. The  $\Delta K=K^+-K''=0$  transitions are dominant, each of the  $\Delta N$  lines consisting of many closely spaced  $\Delta K$  sub band lines. This is confirmed by computations also and the  $\Delta K=\pm 2$  sub bands are calculated to be less than 10% in intensity and are not labeled. The low energy side of the spectrum is not well understood. In methyl radical, transitions with negative  $\Delta N$  have greater intensity due to rotational auto ionization of Rydberg states converging onto rotationally excited states of the ion just as in diatomics.

### Propargyl radical

The propargyl radical, C<sub>3</sub>H<sub>3</sub>, a central intermediate in the formation of soot, and is seen in flames. It plays a role in interstellar chemistry as a precursor to propadienylidene, H<sub>2</sub>CCC, through low energy electron attachment. The ZEKE of propargyl radical is shown in the Figure 7.

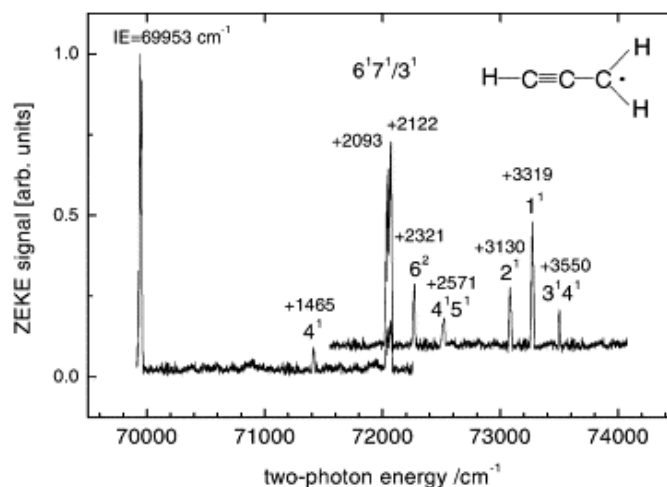


**Figure 7-** The ZEKE –spectrum of propargyl radical.

## Allyl Radical

As the best understood hydrocarbon radical, considerable interest was on the dynamics of allyl. The primary photo physical process upon excitation using photons were studied by time-resolved PES. Being a C<sub>3</sub> hydrocarbon, its chemistry is also of relevance in combustion processes. The allyl is considered to be an intermediate in the formation of soot and polyaromatic hydrocarbons. The ZEKE-spectra were recorded through various vibrational levels of the resonant intermediate B<sup>2</sup>A<sub>1</sub>, C<sup>2</sup>B<sub>1</sub> and D<sup>2</sup>B<sub>2</sub> states. This is important because the lifetimes of these states were measured to be on the order of 20 ps and less. Two ZEKE-spectra are given below in Figure 8 ; the upper one shows the spectrum recorded in a [1+1'] through the C 0<sub>0</sub><sup>0</sup> band, in the lower one the [2+1'] spectrum recorded through the B 0<sub>0</sub><sup>0</sup> states. The [1+1'] spectrum is simple and is dominated by a single transition into the ionic origin band. From FC considerations a simple spectrum is expected since the geometry of the C-state is very similar to the theoretical state. Only the fundamental of the C---C---C bending vibration  $\nu_7^+$  appears weakly in addition due to the slight decrease in the CCC angle upon ionization.

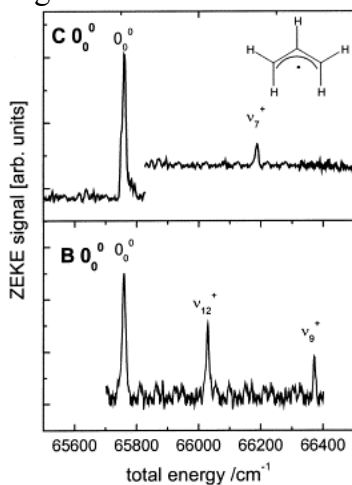


**Figure 8**-The ZEKE-Spectrum of allyl radical, recorded by [1+1'] excitation through the C-state origin.

## NH Radicals

The spectrum of the NH radical is given in Figure 8. Formally NH, or imidogen, with its X<sup>3</sup>Σ<sup>-</sup> ground state is not a radical, but is a simplest nitrene. It is produced by photolysis from HN<sub>3</sub>, giving electronically excited NH in its <sup>1</sup>Δ state. The experimental spectrum obtained by [2+1] REMPI through the f<sup>1</sup>Π (3pσ) v'=0, N'=13 Rydberg state is given on the left-hand side of Figure 9.

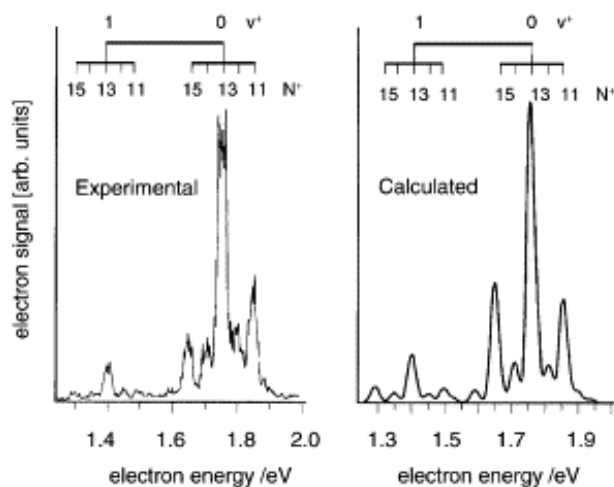


**Figure 9-** The Experimental (Left- hand trace) and ab initio calculated (right-hand trace) conventional photo-electron spectra of NH radicals.

Transitions into the  $v^+=1$  state are less compared to transitions into the  $v^+=0$  state, because of the similar geometry of intermediate state and cation. Notably the spectrum is dominated by even  $\Delta N$  transitions ( $\Delta N=0, \pm 2$ ), even though ionization of a p-electron should be associated with odd  $\Delta N$  transitions due to parity conservation.

The radicals are generated using photons in the ionization region, leading to vibrationally and rotationally hot radicals. Spectral complication is avoided by intermediate state selection using resonant multiphoton method.



### Alkoxy radical ( $\text{R}=\text{CH}_3$ ).

The structure and properties of alkoxy radicals are well studied due to their performance in the combustion processes, interstellar and atmospheric chemistry and as intermediate in hydrocarbon reactions. Due to their small structure, it is good for the theoretical studies. Eg. Methoxy radical

Consider the ground state of  $\text{CH}_3\text{O}$  radical, it is a closed shell anion with  $\text{C}_{3v}$  symmetry having a two-fold degeneracy in its  $\text{C}_{3v}$  geometry. This leads to Jahn- Teller phenomenon. The two non-bonding p orbitals highly localized on the oxygen atom constitute the highest occupied MO. An electron from  $\text{P}_x$  or  $\text{P}_y$  orbital, gives two energetically equivalent configurations for the radical. A schematic representation of these degenerate orbitals is shown in the figure 10. The degenerate electronic states coupled with  $\text{C}_{3v}$  geometry of the radical causes the Jahn-Teller effects in this radical.

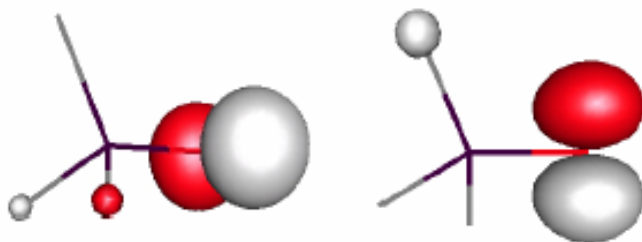


**Figure 10-** Schematic representation of two degenerate highest occupied molecular orbitals of  $\text{CH}_3\text{O}$  radical.

### Photoelectron spectrum of CH<sub>3</sub>O

The ground state of the CH<sub>3</sub>O radical has two-fold degeneracy in its C<sub>3v</sub> configuration leading to Jahn-Teller effects: To minimize the energy, the radical will distort, thus decreasing the C<sub>3v</sub> symmetry and lifting the degeneracy. CH<sub>3</sub>O radical has six vibrational modes, out of the six modes, three are symmetric **a**<sub>1</sub> modes:  $\gamma_1$  CH stretch,  $\gamma_2$  umbrella, and  $\gamma_3$  CO stretch; and three are asymmetric *e* modes:  $\gamma_4$  CH stretch,  $\gamma_5$  HCH scissors, and  $\gamma_6$  methyl rock, which involves movement of the oxygen off the C<sub>3v</sub> axis toward one of the hydrogens. The symmetric modes do not provide the distortion which is enough to remove the degeneracy and lower the energy, and thus only the asymmetric *e* vibrational modes can be Jahn-Teller active. The methoxy radical is known to exhibit a “dynamic” Jahn-Teller effect, where the zero-point energies of the vibrations are greater than the stabilization energy of the Jahn-Teller distortion. So the distortion is not large enough to make a permanent change from C<sub>3v</sub> to C<sub>s</sub> symmetry and must be treated as a vibronic coupling problem where the asymmetric vibrational *e* modes couple to the degenerate E electronic states.

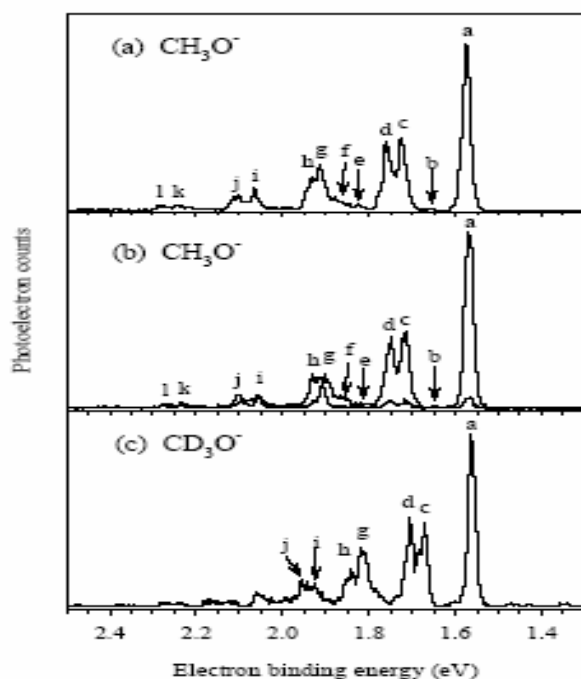


**Figure 11-** a) Magic angle photoelectron spectrum of CH<sub>3</sub>O radical taken at 300K sample temperature. (b) 300K photoelectron spectrum taken at 90° (heavy line) and 0° (light line) polarization angles with respect to electron detection axis. (c) Magic angle photoelectron spectrum of CD<sub>3</sub>O radical at 300K sample temperature, DOO radical subtracted

The room temperature magic angle and 0° and 90° photoelectron spectra for CH<sub>3</sub>O radical are shown in Figure 11a and b, respectively. Peak “a” is assigned as the <sup>0</sup>0<sub>0</sub> transition that gives  $EA(\text{CH}_3\text{O}) = 1.572 \pm 0.004$  eV. The magic angle spectrum depicts what appears at first glance to be a regular Franck-Condon progression of doublets in peaks a, c and d, g and h, i and j, and k and l. Closer examination of the spacings,

however, shows that this is not the case. The spacings between the peaks, c and d, g and h, i and j, and k and l are  $255\text{ cm}^{-1}$ ,  $155\text{ cm}^{-1}$ ,  $365\text{ cm}^{-1}$ , and  $355\text{ cm}^{-1}$ , and the spacing between peaks a and c, c and g, g and i, and I and k are  $1210\text{ cm}^{-1}$ ,  $1530\text{ cm}^{-1}$ ,  $1195\text{ cm}^{-1}$ , and  $1400\text{ cm}^{-1}$ , respectively. Also there are the relatively weak peaks b and e whose photoelectron angular distributions are different from the other peaks in the spectrum. Peaks a, c, d, f, and h show similarities in behavior in the  $90^\circ$  and  $0^\circ$  polarization scans in that their intensities are heavily weighted in the  $90^\circ$  direction (Figure 11-b).

This is clearly seen from the asymmetry parameter values ( $\beta$  of about  $-1$ ) for these peaks listed in Table 11-a. The opposite is true for peaks b and e, whose  $\beta$  values are closer to  $+1$ . All of these values are tabulated and represented in figure 12

Peak	Position ( $\text{cm}^{-1}$ )	$\beta$	Assignment
a	0	-0.9	$0\ 0_0^0$ (E)
b	$630 \pm 10$	$\geq 1.2$	$652\ 6_0^1$ ( $A_1$ )
c	$1210 \pm 10$	-0.9	$1198\ 6_0^1$ (E)
d	$1465 \pm 10$	-0.8	$1490\ 5_0^1$ (E)
e	$2015 \pm 30$	$\geq 1.0$	$2018\ 2_0^1 6_0^1$ ( $A_1$ )
f	$2450 \pm 90$	-0.8	$2432\ 2_0^1 3_0^1$ (E)
			$2441\ 5_0^1 6_0^1$ (E)
			$2488\ 6_0^1$ (E)
g	$2740 \pm 10$	-0.2	$2730\ 5_0^1$ (E)
			2750 ?
			$2760\ 2_0^1 5_0^1$ ( $A_1$ )
h	$2895 \pm 10$	-0.7	$2862\ [5_0^1 / 4_0^1]$ (E)
i	$3935 \pm 10$	-0.1	-
j	$4300 \pm 10$	-0.3	-
k	$5335 \pm 30$	-0.1	-
l	$5690 \pm 15$	-0.1	-

**Figure 12-** Peak position, asymmetry  $\beta$  values and assignments for the photoelectron spectrum of  $\text{CH}_3\text{O}$  radical. Errors on  $\beta$  values are  $\pm 1$

### Conclusion

- Photoelectron spectroscopy may be used as analytical tool.
- Some thermodynamical parameters like Binding Energy of radicals can be calculated using PES.
- Information about the nature of the orbital from which electron is coming out can be known.
- We can study the structural relationship between radicals and radical cations.

### References

- High-resolution photoelectron spectroscopy of radicals
- Institute of Physikalische Chemie der University- Germany
- J. Am. Chem. SOC., Vol. 106, No. 14, 1984 3921
- J Chem. Phys, Vol 110, No 1, 1999.
- Thesis from US